AIMS Mathematics, 8(6): 13503–13524.
DOI: 10.3934/math.2023685
Received: 13 January 2023
Revised: 08 March 2023
Accepted: 15 March 2023
Published: 07 April 2023

http://www.aimspress.com/journal/Math

Research article

On efficient numerical approaches for the study of the interactive dynamics of fractional eco-epidemiological models

Reny George[1,2], Shahram Rezapour[3,4,*], Mohammed Shaaf Alharthi[5], A. F. Aljohani[6,7] and B. Günay[8,*]

[1] Department of Mathematics, College of Science and Humanities in Al-Kharj, Prince Sattam Bin Abdulaziz University, Al-Kharj 11942, Saudi Arabia

[2] Department of Mathematics and Computer Science, St. Thomas College, Bhilai 49006, India

[3] Department of Mathematics, Kyung Hee University, Kyungheedae-ro 26, Dongdaemun-gu, Seoul, Republic of Korea

[4] Department of Medical Research, China Medical University Hospital, China Medical University, Taichung, Taiwan

[5] Department of Mathematics and Statistics, College of Science, Taif University, P. O. Box 11099, Taif 21944, Saudi Arabia

[6] Department of Mathematics, Faculty of Science, University of Tabuk, Tabuk, Saudi Arabia

[7] Department of Mathematical Sciences, George Mason University, Virginia, USA

[8] Faculty of Engineering and Natural Sciences, Bahçeşehir University, Istanbul 34349, Turkey

* **Correspondence:** Emails: rezapourshahram@yahoo.ca, bezgunay@gmail.com.

Abstract: The present study aims to consider a mathematical eco-epidemiological model involving two fractional operators. To this end, we provide approximate solutions to these fractional systems through the application of a numerical technique that is based on the rule of product integration. This feature contributes greatly to the efficiency and effectiveness of both methods. We have also presented some theoretical discussions related to the equilibrium points of the system. Further, several numerical simulations are presented in order to illustrate the impact of choosing different parameters on the dynamics of the model. It is demonstrated that the obtained numerical results are completely consistent with the expected theoretical results. Moreover, both techniques can be used to solve other problems in epidemiology and describe other problems in the future. The article's model has never been studied via the employed fractional operators, and this is a distinct point for our work and other existing research.

Keywords: numerical interactions; explicit and implicit schemes; extinction; sensitivity analysis
Mathematics Subject Classification: 26A33, 37N25, 74S30, 91B50

1. Introduction

A great deal of attention has been paid to the use of mathematical tools in recent years to better describe phenomena in the world, such as nonlinear optics [1], network analysis [2], biomedical signal processing [3], mathematical modelling of human liver [4], medical imaging [5, 6], neural networks [7], optimal control [8], a diffusive epidemic model [9], chemical signal concentration [10], attraction-repulsion [11], control theory [12], signal advancement [13], computational approaches in medicine [14], nanoscience [15], artificial intelligence [16], fractional mathematical model [17], wave propagation [18], and applied mathematical analysis [19]. These eras of research have attracted the attention of many scholars in both science and engineering disciplines and led to the development of many efficient numerical methods. For example, deep learning technique in [20], the Lyapunov functional approach in [21], convolutional neural network in [22], interpretive structural modeling in [23], variational methods in [24], fractal concepts in [25], the Monte Carlo analysis in [26], wave filters in [27, 28]. Other methodologies include optical waveguides in [29], optimization methods in [30], high-frequency measurements in [31], quantitative evaluations in [32], carbon nanotubes computations in [33], microfluidics in [34, 35], classification algorithms in [36]. For more applications, please refer to [37–39].

The purpose of this article is to examine an eco-epidemiological model that simulates how diseases spread in a natural environment under the influence of several factors. Recently, these types of models have gained increasing attention due to the spread and epidemic of infectious diseases. For instance, the authors of [40] have considered the following eco-epidemiological model:

$$\begin{aligned}
\tfrac{d\mathcal{H}_1(t)}{dt} &= r\mathcal{H}_1(t) - b\mathcal{H}_1^2(t) - c\mathcal{H}_1(t)\mathcal{H}_2(t) - \tfrac{\alpha_1\mathcal{H}_1(t)\mathcal{H}_3(t)}{e+\mathcal{H}_1(t)} - \tfrac{\beta\mathcal{H}_1(t)\mathcal{H}_2(t)}{a+\mathcal{H}_1(t)},\\
\tfrac{d\mathcal{H}_2(t)}{dt} &= \tfrac{\beta\mathcal{H}_1(t)\mathcal{H}_2(t)}{a+\mathcal{H}_1(t)} - \tfrac{\alpha_2\mathcal{H}_3(t)\mathcal{H}_2(t)}{d+\mathcal{H}_2(t)} - \mu\mathcal{H}_2(t),\\
\tfrac{d\mathcal{H}_3(t)}{dt} &= \tfrac{\alpha_1 c_1\mathcal{H}_1(t)\mathcal{H}_3(t)}{e+\mathcal{H}_1(t)} + \tfrac{c_2\alpha_2\mathcal{H}_3(t)\mathcal{H}_2(t)}{d+\mathcal{H}_2(t)} - m\mathcal{H}_3(t),
\end{aligned} \tag{1.1}$$

where $\mathcal{H}_1(t), \mathcal{H}_2(t)$ and $\mathcal{H}_3(t)$ are three state variables that denote susceptible and infected prey and predator, respectively. In [41], the following prey-predator model with Atangana-Baleanu derivative model has been investigated:

$$\begin{aligned}
\tfrac{d\mathcal{H}_1(t)}{dt} &= \mathcal{H}_1(t)\left[1 - \mathcal{H}_1(t) - \beta_{12}\mathcal{H}_2(t)\right] + \delta\mathcal{H}_1(t)\mathcal{H}_3(t),\\
\tfrac{d\mathcal{H}_2(t)}{dt} &= r\mathcal{H}_2(t)\left[1 - \mathcal{H}_2(t) - \beta_{21}\mathcal{H}_1(t)\right] - \tfrac{(1-p)\mathcal{H}_2(t)\mathcal{H}_3(t)}{m_1+(1-p)\mathcal{H}_2(t)},\\
\tfrac{d\mathcal{H}_3(t)}{dt} &= \mathcal{H}_3(t)\left[-m_2 + \tfrac{m_3(1-p)\mathcal{H}_2(t)}{m_1+(1-p)\mathcal{H}_2(t)}\right].
\end{aligned} \tag{1.2}$$

More details of the model can be found in [41].

In [42], a three-species predator-prey model in the presence of prey social behavior given by

$$\begin{aligned}
\tfrac{d\mathcal{H}_1(t)}{dt} &= r\mathcal{H}_1(t)\left(1 - \tfrac{\mathcal{H}_1(t)}{k}\right) - \beta\mathcal{H}_1^{\alpha}(t)\mathcal{H}_2(t) - a\mathcal{H}_1^{\alpha}(t)\mathcal{H}_3(t),\\
\tfrac{d\mathcal{H}_2(t)}{dt} &= \beta\mathcal{H}_1^{\alpha}(t)\mathcal{H}_2(t) - c\mathcal{H}_3(t)\mathcal{H}_2(t) - m\mathcal{H}_2(t),\\
\tfrac{d\mathcal{H}_3(t)}{dt} &= c\mathcal{H}_3(t)\mathcal{H}_2(t) + a\mathcal{H}_1^{\alpha}(t)\mathcal{H}_3(t) - \mu\mathcal{H}_3(t),
\end{aligned} \tag{1.3}$$

has been studied.

Research on infectious diseases has recently attracted a great deal of attention. For instance, the outbreak of vector-host diseases is modeled mathematically in [43] using a fractional model with Caputo-Fabrizio derivative. Other studies include the model for hepatitis B virus (HBV) and hepatitis C virus (HCV) co-infection in [44], prevalence of an infectious disease in a prey and predator system in [45], food chain model in [46], and hand-foot-mouth disease in [47]. During the past few decades, fractional calculus operators have become one of the effective tools for modeling various mathematical, physical and engineering problems. Probably the key reason for the increase in popularity of these operators is that they benefit from memory features as one of their main properties. Considering this valuable attribute of the operators, they are invaluable in biological modeling, since what happens in the present will be heavily influenced by what happened in the past with those variables.

In this paper, we incorporate two fractional operators, the Atangana-Baleanu-Caputo and Caputo-Fabrizio-Caputo, into a novel biological system [48]. These kinds of operators have been employed in many studies so far. However, their use should be accompanied by caution and compliance with some necessary conditions as outlined in [49].

Below is a breakdown of the remaining sections. First, some prerequisites are presented in the second part of this paper, including definitions and properties of fractional operators. The main system of the article is introduced in Section 3. A theoretical analysis of the model is presented in Section 4. The basic ideas for obtaining the numerical techniques for the model are presented in Section 5. In Section 6, we discuss the approximate solutions corresponding to the numerical methods used, as well as their implications. In the last section, we discuss several concluding remarks.

2. An overview of fractional calculus

In this section, first, it is necessary to have a brief overview of some useful preliminary theorems in the field of differential calculus of fractional order.

Definition 2.1. The derivative and integral Caputo type (Cap) operators are respectively given by [50]

$$ {}^{\mathsf{Cap}}\mathcal{D}^{\wp}\mathcal{H}(t) = \frac{1}{\Gamma(k-\wp)}\int_0^t (t-\zeta)^{m-\wp-1}\omega^{(k)}(\zeta)d\zeta, \qquad k-1<\wp\leq k, k\in\mathbb{N}, \tag{2.1} $$

and

$$ {}^{\mathsf{Cap}}\mathcal{I}^{\wp}\mathcal{H}(t) = \frac{1}{\Gamma(\wp)}\int_0^t (t-\zeta)^{\wp-1}\omega(\zeta)d\zeta, \qquad 0<\wp<1. \tag{2.2} $$

Definition 2.2. The derivative and integral Atangana-Baleanu-Caputo (ABC) operators are respectively given by [48]

$$ {}^{\mathsf{ABC}}\mathcal{D}^{\wp}\mathcal{H}(t) = \frac{\mathcal{W}(\wp)}{1-\wp}\int_0^t \mathcal{M}_{\wp}\left[-\frac{\wp}{1-\wp}(t-\zeta)\right]\omega'(\zeta)d\zeta, \quad \wp\in(0,1), \tag{2.3} $$

$$ {}^{\mathsf{ABC}}\mathcal{I}^{\wp}\mathcal{H}(t) = \frac{1-\wp}{\mathcal{W}(\wp)}\mathcal{H}(t) + \frac{\wp}{\mathcal{W}(\wp)\Gamma(\wp)}\int_{t_0}^t (t-\mu)^{\wp-1}\omega(\zeta)d\zeta, \tag{2.4} $$

where

$$ \mathcal{W}(\wp) = 1-\wp+\frac{\wp}{\Gamma(\wp)}, $$

and $\mathcal{M}_{\wp}(\zeta)$ is the Mittag-Leffler function given by

$$\mathcal{M}_{\wp}(t) = \sum_{j=0}^{\infty} \frac{t^j}{\Gamma(1 + j\wp)}. \tag{2.5}$$

After applying the integral operator ABC defined in (2.4) to the differential operator (2.3), one concludes that

$${}^{\mathsf{ABC}}\mathcal{I}^{\wp}\left({}^{\mathsf{ABC}}\mathcal{D}^{\wp}\mathcal{H}(t)\right) = \mathcal{H}(t) - \mathcal{H}(0). \tag{2.6}$$

The Laplace transform corresponding to the ABC operator defined by (2.3) is obtained as

$$\mathcal{L}\left[{}^{\mathsf{ABC}}\mathcal{D}^{\wp}\mathcal{H}(t)\right] = \frac{\mathcal{W}(\wp)}{1-\wp}\frac{s\mathcal{L}\left[\mathcal{H}(t)\right] - s^{\wp-1}\mathcal{H}(0)}{s + \frac{\wp}{1-\wp}}. \tag{2.7}$$

Definition 2.3. The derivative and integral Caputo-Fabrizio-Caputo (CFC) operators are respectively given by [51]

$${}^{\mathsf{CFC}}\mathcal{D}^{\wp}\mathcal{H}(t) = \frac{\mathsf{Q}(\wp)}{k-\wp}\int_0^t \frac{d^k\omega(\zeta)}{d\zeta^k} exp\left[-\frac{\wp}{n-\wp}(t-\zeta)\right]d\zeta, \quad k-1 < \wp \leq k, \tag{2.8}$$

$${}^{\mathsf{CFC}}\mathcal{I}^{\wp}\mathcal{H}(t) = \frac{2(1-\wp)}{(2-\wp)\mathsf{Q}(\wp)}\mathcal{H}(t) + \frac{2\wp}{(2-\wp)\mathsf{Q}(\wp)}\int_0^t \omega(\zeta)d\zeta, \tag{2.9}$$

where

$$\mathsf{Q}(\wp) = \frac{2}{2-\wp}. \tag{2.10}$$

The Laplace transform corresponding to the CFC operator defined by (2.8) is obtained as [41]

$$\mathcal{L}\left[{}^{\mathsf{CFC}}\mathcal{D}^{\wp}\mathcal{H}(t)\right] = \frac{s^{n+1}\mathcal{L}\left[\mathcal{H}(t)\right] - s^n\mathcal{H}(0) - s^{n-1}\mathcal{H}'(0) - \ldots - \mathcal{H}^{(n)}(0)}{s + \wp(1-s)}, \quad n-1 < \wp \leq n. \tag{2.11}$$

3. The main model

The main focus of this paper is to study the mathematical description of interactions between the populations of susceptible and infected prey given by $\mathcal{H}_1(t)$ and $\mathcal{H}_2(t)$, respectively. Moreover, $\mathcal{H}_3(t)$ denotes the predator population. The mathematical description of the interactions of these components is expressed by the following nonlinear system [52]:

$$\begin{aligned}
\tfrac{d\mathcal{H}_1(t)}{dt} &= \tfrac{a\mathcal{H}_1(t)}{1+\kappa\mathcal{H}_3(t)} - d\mathcal{H}_1(t) - b\mathcal{H}_1(t)(\mathcal{H}_1(t) + \mathcal{H}_2(t)) - \beta\mathcal{H}_1(t)\mathcal{H}_2(t),\\
\tfrac{d\mathcal{H}_2(t)}{dt} &= \beta\mathcal{H}_1(t)\mathcal{H}_2(t) - p\mathcal{H}_2(t)\mathcal{H}_3(t) - \delta\mathcal{H}_2(t),\\
\tfrac{d\mathcal{H}_3(t)}{dt} &= cp\mathcal{H}_2(t)\mathcal{H}_3(t) - \mu\mathcal{H}_3(t).
\end{aligned} \tag{3.1}$$

In this model, it is assumed that the only population that is infected by infectious disease is that of the prey. Moreover, infected prey are consumed by predators, while susceptible prey do not fall under

their diet. The parameters of the model are as follows: a represents the birth rate of the susceptible prey, d is used to explain the rate of natural death in susceptible prey, b stands for the density-dependent death rate based on intra-species competition, and β describes the contact rate between the susceptible and the infected prey. Moreover, p shows the attack rate on the infected prey, and the death rate of the infected prey is presented by δ, c demonstrates the conversion coefficient. Also, μ shows the corresponding natural rate of the death for predator populations, and finally, the parameter κ denotes the level of fear which drives anti-predator behavior of the prey [40]. A comprehensive explanation of the formation of this non-linear model can be found in [40].

In this paper, we will apply two more recent definitions of fractional differential calculus in the model presented by (3.1). First, let us replace standard derivatives in the model with the ABC fractional derivative (2.3) to get the following fractional model:

$$\begin{aligned} {}^{\mathsf{ABC}}\mathcal{D}^{\wp}\mathcal{H}_1(t) &= \tfrac{a\mathcal{H}_1(t)}{1+\kappa\mathcal{H}_3(t)} - d\mathcal{H}_1(t) - b(\mathcal{H}_1{}^2(t) + \mathcal{H}_1(t)\mathcal{H}_2(t)) - \beta\mathcal{H}_1(t)\mathcal{H}_2(t), \\ {}^{\mathsf{ABC}}\mathcal{D}^{\wp}\mathcal{H}_2(t) &= \beta\mathcal{H}_1(t)\mathcal{H}_2(t) - p\mathcal{H}_2(t)\mathcal{H}_3(t) - \delta\mathcal{H}_2(t), \\ {}^{\mathsf{ABC}}\mathcal{D}^{\wp}\mathcal{H}_3(t) &= cp\mathcal{H}_2(t)\mathcal{H}_3(t) - \mu\mathcal{H}_3(t), \end{aligned} \tag{3.2}$$

subject to initial conditions

$$(\mathcal{H}_1(t=0), \mathcal{H}_2(t=0), \mathcal{H}_3(t=0)) = (\mathcal{H}_{1,0}, \mathcal{H}_{2,0}, \mathcal{H}_{3,0}) \geq 0.$$

Moreover, by applying the CFC fractional derivative (2.8) in the model, we arrive at the following fractional model:

$$\begin{aligned} {}^{\mathsf{CFC}}\mathcal{D}^{\wp}\mathcal{H}_1(t) &= \tfrac{a\mathcal{H}_1(t)}{1+\kappa\mathcal{H}_3(t)} - d\mathcal{H}_1(t) - b(\mathcal{H}_1{}^2(t) + \mathcal{H}_1(t)\mathcal{H}_2(t)) - \beta\mathcal{H}_1(t)\mathcal{H}_2(t), \\ {}^{\mathsf{CFC}}\mathcal{D}^{\wp}\mathcal{H}_2(t) &= \beta\mathcal{H}_1(t)\mathcal{H}_2(t) - p\mathcal{H}_2(t)\mathcal{H}_3(t) - \delta\mathcal{H}_2(t), \\ {}^{\mathsf{CFC}}\mathcal{D}^{\wp}\mathcal{H}_3(t) &= cp\mathcal{H}_2(t)\mathcal{H}_3(t) - \mu\mathcal{H}_3(t). \end{aligned} \tag{3.3}$$

4. Mathematical analysis for model

In order to find more analytical intuition of the model (3.2), some related mathematical analyses are collected in this section.

4.1. The basic reproduction number

In this model, the basic reproduction number $\mathcal{R}_0$ for system (3.2) is calculated as [52]

$$\mathcal{R}_0 = \frac{a\beta}{b\delta}. \tag{4.1}$$

4.2. The equilibrium points

The following positive equilibrium points can be calculated for the model (3.2).

- The trivial point of $\mathcal{P}_0 = (0, 0, 0)$.
- The axial point of $\mathcal{P}_1 = \left(\frac{a-d}{b}, 0, 0\right)$. This point exists if we have $a > d$.

- The axial equilibrium point of $\mathcal{P}_2 = \left(\frac{\delta}{\beta}, \frac{a\beta - b\delta - d\beta}{\beta(b+\beta)}, 0\right)$. This point exists if we have $a\beta - b\delta > d\beta$.
- Other equilibrium points $\mathcal{P}_i = (\mathcal{H}_1^*, \mathcal{H}_2^*, \mathcal{H}_3^*)$ of the system can be evaluated by determining the positive solutions of the following nonlinear algebraic system:

$$\begin{aligned} &\tfrac{a\mathcal{H}_1^*}{1+\kappa\mathcal{H}_3^*} - d\mathcal{H}_1^* - b\mathcal{H}_1^*(\mathcal{H}_1^* + \mathcal{H}_2^*) - \beta\mathcal{H}_1^*\mathcal{H}_2^* = 0, \\ &\beta\mathcal{H}_1^*\mathcal{H}_2^* - p\mathcal{H}_2^*\mathcal{H}_3^* - \delta\mathcal{H}_2^* = 0, \\ &cp\mathcal{H}_2^*\mathcal{H}_3^* - \mu\mathcal{H}_3^* = 0. \end{aligned} \tag{4.2}$$

The local stability for these equilibrium points $\mathcal{P}_i = (\mathcal{H}_1^*, \mathcal{H}_2^*, \mathcal{H}_3^*)$ can be explored using the Jacobian matrix as

$$\mathcal{J}(\mathcal{H}_1^*, \mathcal{H}_2^*, \mathcal{H}_3^*) = \begin{bmatrix} \frac{a}{\kappa\mathcal{H}_3^*+1} - d - b\left(2\mathcal{H}_1^* + \mathcal{H}_2^*\right) - \beta\mathcal{H}_2^* & -b\mathcal{H}_1^* - \beta\mathcal{H}_1^* & -\frac{a\mathcal{H}_1^*\kappa}{\left(\kappa\mathcal{H}_3^*+1\right)^2} \\ \beta\mathcal{H}_2^* & \beta\mathcal{H}_1^* - p\mathcal{H}_3^* - \delta & -p\mathcal{H}_2^* \\ 0 & cp\mathcal{H}_3^* & cp\mathcal{H}_2^* - \mu \end{bmatrix}. \tag{4.3}$$

4.3. The existence of the solution for the model (3.2)

To this end, let us employ the ABC integral operator (2.4) on the system (3.2). Then, we get

$$\begin{aligned} \mathcal{H}_1(t) - \mathcal{H}_1(0) &= \frac{1-\wp}{\mathcal{W}(\wp)}\mathcal{Q}_1(\mathbf{H(t)}) + \frac{\wp}{\mathcal{W}(\wp)\Gamma(\wp)}\int_0^t (t-\zeta)^{\wp-1}\mathcal{Q}_1(\mathbf{H}(\zeta))d\zeta, \\ \mathcal{H}_2(t) - \mathcal{H}_2(0) &= \frac{1-\wp}{\mathcal{W}(\wp)}\mathcal{Q}_2(\mathbf{H(t)}) + \frac{\wp}{\mathcal{W}(\wp)\Gamma(\wp)}\int_0^t (t-\zeta)^{\wp-1}\mathcal{Q}_2(\mathbf{H}(\zeta))d\zeta, \\ \mathcal{H}_3(t) - \mathcal{H}_3(0) &= \frac{1-\wp}{\mathcal{W}(\wp)}\mathcal{Q}_3(\mathbf{H(t)}) + \frac{\wp}{\mathcal{W}(\wp)\Gamma(\wp)}\int_0^t (t-\zeta)^{\wp-1}\mathcal{Q}_3(\mathbf{H}(\zeta))d\zeta, \end{aligned} \tag{4.4}$$

where $\mathbf{H(t)} = [\mathcal{H}_1(t), \mathcal{H}_2(t), \mathcal{H}_3(t)]$, and also we define

$$\begin{aligned} \mathcal{Q}_1(\mathbf{H(t)}) &= \tfrac{a\mathcal{H}_1(t)}{1+\kappa\mathcal{H}_3(t)}\mathcal{H}_1(t) - d - b\mathcal{H}_1(t)(\mathcal{H}_1(t) + \mathcal{H}_2(t)) - \beta\mathcal{H}_1(t)\mathcal{H}_2(t), \\ \mathcal{Q}_2(\mathbf{H(t)}) &= \beta\mathcal{H}_1(t)\mathcal{H}_2(t) - p\mathcal{H}_2(t)\mathcal{H}_3(t) - \delta\mathcal{H}_2(t), \\ \mathcal{Q}_3(\mathbf{H(t)}) &= cp\mathcal{H}_2(t)\mathcal{H}_3(t) - \mu\mathcal{H}_3(t). \end{aligned} \tag{4.5}$$

Define

$$\mathbf{M(H(t))} = [\mathcal{Q}_1(\mathbf{H(t)}), \mathcal{Q}_2(\mathbf{H(t)}), \mathcal{Q}_3(\mathbf{H(t)})],$$

and moreover

$$\mathbf{H}_0 = [\mathcal{H}_1(0), \mathcal{H}_2(0), \mathcal{H}_3(0)].$$

Using these assumptions, Eq (4.4) can be rewritten as

$$\mathbf{H}(t) - \mathbf{H}_0 = \frac{1-\wp}{\mathcal{W}(\wp)}\mathbf{M(H(t))} + \frac{\wp}{\mathcal{W}(\wp)\Gamma(\wp)}\int_0^t (t-\zeta)^{\wp-1}\mathbf{M}(\mathbf{H}(\zeta))d\zeta. \tag{4.6}$$

Then, from (4.6) along with $\mathbf{H}_0(t) = \mathbf{H}_0$, the following recursive structure is conceivable:

$$\mathbf{H}_n(t) - \mathbf{H}_0 = \frac{1-\wp}{\mathcal{W}(\wp)}\mathbf{M}(\mathbf{H}_{n-1}(t)) + \frac{\wp}{\mathcal{W}(\wp)\Gamma(\wp)}\int_0^t (t-\zeta)^{\wp-1}\mathbf{M}(\mathbf{H}_{n-1}(\zeta))d\zeta. \tag{4.7}$$

Considering Eq (4.7), we will have

$$\begin{aligned}\mathbf{H}_n(t)-\mathbf{H}_{n-1}(t) &= \frac{1-\wp}{\mathcal{W}(\wp)}\left[\mathbf{M}(\mathbf{H}_{n-1}(t))-\mathbf{M}(\mathbf{H}_{n-2}(t))\right] &(4.8)\\ &+ \frac{\wp}{\mathcal{W}(\wp)\Gamma(\wp)}\int_0^t (t-\zeta)^{\wp-1}\left[\mathbf{M}(\mathbf{H}_{n-1}(\zeta))-\mathbf{M}(\mathbf{H}_{n-2}(\zeta))\right]d\zeta. &(4.9)\end{aligned}$$

In this position, we define

$$\varrho_n(t)=\mathbf{H}_n(t)-\mathbf{H}_{n-1}(t).$$

Then, it follows that

$$\mathbf{H}_n(t)=\sum_{i=0}^{n}\varrho_i(t). \tag{4.10}$$

As a result, one gets

$$\begin{aligned}\|\varrho_n(t)\| &= \|\mathbf{H}_n(t)-\mathbf{H}_{n-1}(t)\|,\\ \|\varrho_n(t)\| &= \|\frac{1-\wp}{\mathcal{W}(\wp)}\left[\mathbf{M}(\mathbf{H}_{n-1}(t))-\mathbf{M}(\mathbf{H}_{n-2}(t))\right] &(4.11)\\ &+ \frac{\wp}{\mathcal{W}(\wp)\Gamma(\wp)}\int_0^t (t-\zeta)^{\wp-1}\left[\mathbf{M}(\mathbf{H}_{n-1}(\zeta))-\mathbf{M}(\mathbf{H}_{n-2}(\zeta))\right]d\zeta\|.\end{aligned}$$

Hence, we have

$$\begin{aligned}\|\varrho_n(t)\| &\le \frac{1-\wp}{\mathcal{W}(\wp)}\|\mathbf{M}(\mathbf{H}_{n-1}(t))-\mathbf{M}(\mathbf{H}_{n-2}(t))\|\\ &+ \frac{\wp}{\mathcal{W}(\wp)\Gamma(\wp)}\int_0^t (t-\zeta)^{\wp-1}\|\mathbf{M}(\mathbf{H}_{n-1}(\zeta))-\mathbf{M}(\mathbf{H}_{n-2}(\zeta))\|d\zeta. &(4.12)\end{aligned}$$

Now, our main assumption will be that the nonlinear operator $\mathbf{M}$ has the Leibniz condition, so we can write

$$\|\varrho_n(t)\|\le\frac{1-\wp}{\mathcal{W}(\wp)}\mathbf{L}\|\mathbf{H}_{n-1}(t)-\mathbf{H}_{n-2}(t)\|+\frac{\wp\mathbf{L}}{\mathcal{W}(\wp)\Gamma(\wp)}\int_0^t(t-\zeta)^{\wp-1}\|\mathbf{H}_{n-1}(t)-\mathbf{H}_{n-2}(t)\|d\zeta.$$

Consequently, we derive the following inequality:

$$\|\varrho_n(t)\|\le\frac{1-\wp}{\mathcal{W}(\wp)}\mathbf{L}\|\varrho_{n-1}(t)\|+\frac{\wp\mathbf{L}}{\mathcal{W}(\wp)\Gamma(\wp)}\int_0^t(t-\zeta)^{\wp-1}\|\varrho_{n-1}(t)\|d\zeta.$$

Further, replacing $\|\varrho_{n-1}(t)\|$, one arrives at

$$\|\varrho_n(t)\|\le\left(\frac{1-\wp}{\mathcal{W}(\wp)}\mathbf{L}+\frac{\wp\mathbf{L}t^{\wp}}{\mathcal{W}(\wp)\Gamma(\wp+1)}\right)^2\|\varrho_{n-2}(t)\|.$$

Also, it reads

$$\|\varrho_n(t)\|\le\left(\frac{1-\wp}{\mathcal{W}(\wp)}\mathbf{L}+\frac{\wp\mathbf{L}t^{\wp}}{\mathcal{W}(\wp)\Gamma(\wp+1)}\right)^3\|\varrho_{n-3}(t)\|.$$

And, finally, we obtain

$$\begin{aligned} \|\varrho_n(t)\| &\leq \left(\frac{1-\wp}{\mathcal{W}(\wp)}\mathbf{L} + \frac{\wp \mathbf{L} t^{\wp}}{\mathcal{W}(\wp)\Gamma(\wp+1)}\right)^n \|\varrho_0(t)\| \\ &\leq \left(\frac{1-\wp}{\mathcal{W}(\wp)} + \frac{\wp t^{\wp}}{\mathcal{W}(\wp)\Gamma(\wp+1)}\right)^n \mathbf{L}^n max_{t\in[0,T]}\mathbf{H}_0(t). \end{aligned} \tag{4.13}$$

Now, let us define

$$\mathbf{H}(t) = \sum_{i=0}^{n} \varrho_i(t). \tag{4.14}$$

In addition, according to the $\mathbf{H}(t)$ structure, it holds that

$$\mathbf{H}(t) = \mathbf{H}_n(t) + \theta_n(t), \tag{4.15}$$

where $\theta_n(t) \to 0$ when $n(t) \to \infty$. Thus,

$$\mathbf{H}(t) - \mathbf{H}_n(t) = \frac{1-\wp}{\mathcal{W}(\wp)}\mathbf{M}(\mathbf{H}(t) - \theta_n(t)) + \frac{\wp}{\mathcal{W}(\wp)\Gamma(\wp)}\int_0^t (t-\zeta)^{\wp-1}\mathbf{M}(\mathbf{H}(\zeta) - \mu_n(\zeta))d\zeta. \tag{4.16}$$

Now, we can write

$$\begin{aligned} \mathbf{H}(t) &- \mathbf{H}_0 - \frac{1-\wp}{\mathcal{W}(\wp)}\mathbf{M}(\mathbf{H}(t) - \theta_n(t)) - \frac{\wp}{\mathcal{W}(\wp)\Gamma(\wp)}\int_0^t (t-\zeta)^{\wp-1}\mathbf{M}(\mathbf{H}(\zeta) - \mu_n(\zeta))d\zeta \\ &= \theta_n(t) + \frac{1-\wp}{\mathcal{W}(\wp)}\left[\mathbf{M}(\mathbf{H}(t) - \theta_n(t)) - \mathbf{M}(\mathbf{H}(t))\right] \\ &- \frac{\wp}{\mathcal{W}(\wp)\Gamma(\wp)}\int_0^t (t-\zeta)^{\wp-1}\Big[\mathbf{M}(\mathbf{H}(\zeta) - \mu_n(\zeta)) - \mathbf{M}(\mathbf{H}(\zeta))\Big]d\zeta. \end{aligned} \tag{4.17}$$

After applying the norm of the above equation, we will have

$$\begin{aligned} \|\mathbf{H}(t) - \mathbf{H}_0(t) &- \frac{1-\wp}{\mathcal{W}(\wp)}\mathbf{M}(\mathbf{H}(t)) + \frac{\wp}{\mathcal{W}(\wp)\Gamma(\wp)}\int_0^t (t-\zeta)^{\wp-1}\mathbf{M}(\mathbf{H}(\zeta)d\zeta\| \\ &\leq \|\theta_n(t)\| + \frac{1-\wp}{\mathcal{W}(\wp)}\|\mathbf{M}(\mathbf{H}(\zeta) - \mu_n(\zeta)) - \mathbf{M}(\mathbf{H}(\zeta))\| \\ &+ \frac{\wp}{\mathcal{W}(\wp)\Gamma(\wp)}\int_0^t (t-\zeta)^{\wp-1}\|\mathbf{M}(\mathbf{H}(\zeta) - \mu_n(\zeta)) - \mathbf{M}(\mathbf{H}(\zeta))\|d\zeta \\ &\leq \|\theta_n(t)\| + \frac{1-\wp}{\mathcal{W}(\wp)}\mathbf{L}\|\theta_{n-1}(t)\| + \frac{\wp t^{\wp}}{\mathcal{W}(\wp)\Gamma(\wp+1)}\mathbf{L}\|\theta_{n-1}(t)\|. \end{aligned}$$

For $n \to \infty$, we have

$$\mathbf{H(t)} - \mathbf{H}_0 = \frac{1-\wp}{\mathcal{W}(\wp)}\mathbf{M}(\mathbf{H(t)}) + \frac{\wp}{\mathcal{W}(\wp)\Gamma(\wp)}\int_0^t (t-\zeta)^{\wp-1}\mathbf{M}(\mathbf{H}(\zeta))d\zeta. \tag{4.18}$$

This will be the result for the existence of the solution.

4.4. The uniqueness of the solution

In order to prove the uniqueness of the solution, let us assume that $\mathbf{H}_1(t)$ and $\mathbf{H}_2(t)$ are two solutions to the problem. So, we have

$$\begin{aligned}
\|\mathbf{H}_1(t) - \mathbf{H}_2(t)\| &\leq \frac{1-\wp}{\mathcal{W}(\wp)}\mathbf{L}\|\mathbf{H}_1(t) - \mathbf{H}_2(t)\| + \frac{\wp \mathbf{L} t^{\wp}}{\mathcal{W}(\wp)\Gamma(\wp+1)}\|\mathbf{H}_1(t) - \mathbf{H}_2(t)\| \\
&\leq \left(\frac{1-\wp}{\mathcal{W}(\wp)}\mathbf{L} + \frac{\wp \mathbf{L} t^{\wp}}{\Theta(1+\wp)\Gamma(\wp)}\right)\|\mathbf{H}_1(t) - \mathbf{H}_2(t)\| \\
&\vdots \\
&\leq \left(\frac{1-\wp}{\mathcal{W}(\wp)}\mathbf{L} + \frac{\wp \mathbf{L} t^{\wp}}{\Theta(1+\wp)\Gamma(\wp)}\right)^{n}\|\mathbf{H}_1(t) - \mathbf{H}_2(t)\|.
\end{aligned}$$

So, if we have

$$\frac{1-\wp}{\mathcal{W}(\wp)}\mathbf{L} + \frac{\wp \mathbf{L} t^{\wp}}{\Theta(1+\wp)\Gamma(\wp)} < 1,$$

then by taking $n \to \infty$, we obtain

$$\left(\frac{1-\wp}{\mathcal{W}(\wp)}\mathbf{L} + \frac{\wp \mathbf{L} t^{\wp}}{\Theta(1+\wp)\Gamma(\wp)}\right)^{n} \to 0.$$

Thus, $\|\mathbf{H}_1(t) - \mathbf{H}_2(t)\| = 0$ holds. Therefore, $\mathbf{H}_1(t) = \mathbf{H}_2(t)$ results.

5. Numerical techniques

Along with providing new differential operators in fractional calculus, the most important concern will always be the design of efficient approximate algorithms for solving those problems numerically. Thus, there is always a numerical method that needs to be developed for each new definition of an operator. There are advantages, limitations, and requirements associated with each of these numerical methods. Our objective in this section is to design two numerical techniques using the definition of the product integration rule (PI), as outlined in [53].

5.1. A numerical scheme for ABC *fractional problem* (3.2)

To extract an efficient numerical technique for ABC fractional problems, we take the following fractional Cauchy problem:

$$^{\mathsf{ABC}}\mathcal{D}^{\wp}\mathcal{H}(t) = \mathcal{N}(t, \mathcal{H}(t)). \tag{5.1}$$

Based on the application of the ABC fractional integral definition in Eq (2.4) on Eq (5.1), we derive the integral equation as follows:

$$\mathcal{H}(t) - \mathcal{H}(t_0) = \frac{1-\wp}{\mathcal{W}(\wp)}\mathcal{N}(t, \mathcal{H}(t)) + \frac{\wp}{\mathcal{W}(\wp)\Gamma(\wp)}\int_{t_0}^{t}(t-\zeta)^{\wp-1}\mathcal{N}(\zeta, \mathcal{H}(\zeta))d\zeta. \tag{5.2}$$

Setting $t = t_n = t_0 + n\Delta t$ in Eq (5.2) yields

$$\mathcal{H}(t_n) = \mathcal{H}(t_0) + \frac{1-\wp}{\mathcal{W}(\wp)}\mathcal{N}(t_n, \mathcal{H}(t_n)) + \frac{\wp}{\mathcal{W}(\wp)\Gamma(\wp)}\sum_{i=0}^{n-1}\int_{t_i}^{t_{i+1}}(t_n-\zeta)^{\wp-1}\mathcal{N}(\zeta, \mathcal{H}(\zeta))d\zeta. \tag{5.3}$$

Now, a linearized form of $\mathcal{N}(\zeta, \mathcal{H}(\zeta))$ is considered as follows:

$$\mathcal{N}(\zeta, \mathcal{H}(\zeta)) \approx \mathcal{N}(t_{i+1}, \mathcal{H}_{i+1}) + \frac{\zeta - t_{i+1}}{\Delta t} \left(\mathcal{N}(t_{i+1}, \mathcal{H}_{i+1}) - \mathcal{N}(t_i, \mathcal{H}_i)\right), \ \zeta \in [t_i, t_{i+1}], \tag{5.4}$$

where $\mathcal{H}_i = \mathcal{H}(t_i)$.

Using (5.4) in (5.3), and also by doing some algebraic calculations, we obtain [54–56]:

$$\mathcal{H}_n = \mathcal{H}_0 + \frac{\wp \Delta t}{\mathcal{W}(\wp)} \left(\nu_n \mathcal{N}(t_0, \mathcal{H}_0) + \sum_{i=1}^{n} \zeta_{n-i} \mathcal{N}(t_i, \mathcal{H}_i) \right), \ n \geq 1, \tag{5.5}$$

where

$$\begin{aligned} \sigma_n &= \frac{(-1+n)^{\wp+1} - n(-1+n-\wp)}{\Gamma(\wp+2)}, \\ \zeta_i &= \begin{cases} \frac{1-\wp}{\wp \Delta t} + \frac{1}{\Gamma(\wp+2)}, i = 0, \\ \frac{(i-1)^{\wp+1} - 2i^{\wp+1} + (i+1)^{\wp+1}}{\Gamma(\wp+2)}, i = 1, 2, \ldots, n-1. \end{cases} \end{aligned} \tag{5.6}$$

As a result of (5.5) and (5.6), one can effectively assess the approximate solution to the fractional system (5.1). In particular, to approximate the problem (3.2), we will have

$$\begin{aligned} \mathcal{H}_{1,n} &= \mathcal{H}_{1,0} + \frac{\wp \Delta t}{\mathcal{W}(\wp)} \Bigg[\sigma_n \Big(\frac{a\mathcal{H}_{1,0}}{1 + \kappa \mathcal{H}_{3,0}} \mathcal{H}_{1,0} - d - b\mathcal{H}_{1,0}(\mathcal{H}_{1,0} + \mathcal{H}_{2,0}) - \beta \mathcal{H}_{1,0} \mathcal{H}_{2,0} \Big) \\ &\quad + \sum_{i=0}^{n} \zeta_{n-i} \Big(\frac{a\mathcal{H}_{1,i}}{1 + \kappa \mathcal{H}_{3,i}} \mathcal{H}_{1,i} - d - b\mathcal{H}_{1,i}(\mathcal{H}_{1,i} + \mathcal{H}_{2,i}) - \beta \mathcal{H}_{1,i} \mathcal{H}_{2,i} \Big) \Bigg], \\ \mathcal{H}_{2,n} &= \mathcal{H}_{2,0} + \frac{\wp \Delta t}{\mathcal{W}(\wp)} \Bigg[\sigma_n \Big(\beta \mathcal{H}_{1,0} \mathcal{H}_{2,0} - p\mathcal{H}_{2,0} \mathcal{H}_{3,0} - \delta \mathcal{H}_{2,0} \Big) \\ &\quad + \sum_{i=0}^{n} \zeta_{n-i} \Big(\beta \mathcal{H}_{1,i} \mathcal{H}_{2,i} - p\mathcal{H}_{2,i} \mathcal{H}_{3,i} - \delta \mathcal{H}_{2,i} \Big) \Bigg], \\ \mathcal{H}_{3,n} &= \mathcal{H}_{3,0} + \frac{\wp \Delta t}{\mathcal{W}(\wp)} \Bigg[\sigma_n \Big(cp\mathcal{H}_{2,0} \mathcal{H}_{3,0} - \mu \mathcal{H}_{3,0} \Big) + \sum_{i=0}^{n} \zeta_{n-i} \Big(cp\mathcal{H}_{2,i} \mathcal{H}_{3,i} - \mu \mathcal{H}_{3,i} \Big) \Bigg]. \end{aligned} \tag{5.7}$$

These resulting schemes have implicit structures which can be solved utilizing efficient techniques in solving systems of nonlinear algebraic equations like Newton's method.

5.2. A numerical scheme for CFC *fractional problem* (3.3)

In this part, to extract a numerical scheme for CFC fractional problem (3.3), we study the following fractional system:

$$^{\mathsf{CFC}}\mathcal{D}^{\wp} \mathcal{H}(t) = \mathcal{N}(t, \mathcal{H}(t)). \tag{5.8}$$

Utilizing the corresponding fractional integral operator (2.9) on both sides of (5.8) yields

$$\mathcal{H}(t) - \mathcal{H}(0) = \frac{1 - \wp}{\mathsf{Q}(\wp)} \mathcal{N}(t, \mathcal{H}(t)) + \frac{\wp}{\mathsf{Q}(\wp)} \int_0^t \mathcal{N}(\zeta, \mathcal{H}(\zeta)) d\zeta. \tag{5.9}$$

Taking $t = t_{n+1}$ in (5.9), one has

$$\mathcal{H}(t_{n+1}) - \mathcal{H}(0) = \frac{(2-\wp)(1-\wp)}{2}\mathcal{N}(t_n, \mathcal{H}(t_n)) + \frac{\wp(2-\wp)}{2}\int_0^{t_{n+1}} \mathcal{N}(\zeta, \mathcal{H}(\zeta))d\zeta, \tag{5.10}$$

and

$$\mathcal{H}(t_n) - \mathcal{H}(0) = \frac{(2-\wp)(1-\wp)}{2}\mathcal{N}(t_{n-1}, \mathcal{H}(t_{n-1})) + \frac{\wp(2-\wp)}{2}\int_0^{t_n} \mathcal{N}(\zeta, \mathcal{H}(\zeta))d\zeta. \tag{5.11}$$

Inserting Eq (5.11) into Eq (5.10), we obtain

$$\begin{aligned}\mathcal{H}(t_{n+1}) = \mathcal{H}(t_n) &+ \frac{(2-\wp)(1-\wp)}{2}\left[\mathcal{N}(t_n, \mathcal{H}(t_n)) - \mathcal{N}(t_{n-1}, \mathcal{H}(t_{n-1}))\right] \\ &+ \frac{\wp(2-\wp)}{2}\int_{t_n}^{t_{n+1}} \mathcal{N}(\zeta, \mathcal{H}(\zeta))d\zeta,\end{aligned} \tag{5.12}$$

where

$$\int_{t_n}^{t_{n+1}} \mathcal{N}(\zeta, \mathcal{H}(\zeta))d\zeta = \frac{3\Delta t}{2}\mathcal{N}(t_n, \mathcal{H}_n) - \frac{\Delta t}{2}\mathcal{N}(t_{n-1}, \mathcal{H}_{n-1}). \tag{5.13}$$

Thus, we get

$$\begin{aligned}\mathcal{H}_{n+1} = \mathcal{H}_n &+ \left[\frac{(2-\wp)(1-\wp)}{2} + \frac{3\Delta t}{4}\wp(2-\wp)\right]\mathcal{N}(t_n, \mathcal{H}_n) \\ &- \left[\frac{(2-\wp)(1-\wp)}{2} + \frac{\Delta t}{4}\wp(2-\wp)\right]\mathcal{N}(t_{n-1}, \mathcal{H}_{n-1}).\end{aligned} \tag{5.14}$$

Accordingly, the following iterative schemes are determined in order to approximate the problem (3.3) in the following manner [57]:

$$\begin{aligned}\mathcal{H}_{1,n+1} = \mathcal{H}_{1,n} &+ \left[\frac{(2-\wp)(1-\wp)}{2} + \frac{3\Delta t}{4}\wp(2-\wp)\right]\begin{pmatrix} \frac{a\mathcal{H}_{1,n}}{1+\kappa\mathcal{H}_{3,n}}\mathcal{H}_{1,n} - d - \beta\mathcal{H}_{1,n}\mathcal{H}_{2,n} \\ -b\mathcal{H}_{1,n}(\mathcal{H}_{1,n} + \mathcal{H}_{2,n}) \end{pmatrix} \\ &- \left[\frac{(2-\wp)(1-\wp)}{2} + \frac{\Delta t}{4}\wp(2-\wp)\right]\begin{pmatrix} \frac{a\mathcal{H}_{1,n}}{1+\kappa\mathcal{H}_{3,n}}\mathcal{H}_{1,n-1} - d - \beta\mathcal{H}_{1,n-1}\mathcal{H}_{2,n-1} \\ -b\mathcal{H}_{1,n-1}(\mathcal{H}_{1,n-1} + \mathcal{H}_{2,n-1}) \end{pmatrix}, \\ \mathcal{H}_{2,n+1} = \mathcal{H}_{2,n} &+ \left[\frac{(2-\wp)(1-\wp)}{2} + \frac{3\Delta t}{4}\wp(2-\wp)\right]\left(\beta\mathcal{H}_{1,n}\mathcal{H}_{2,n} - p\mathcal{H}_{2,n}\mathcal{H}_{3,n} - \delta\mathcal{H}_{2,n}\right) \\ &- \left[\frac{(2-\wp)(1-\wp)}{2} + \frac{\Delta t}{4}\wp(2-\wp)\right]\left(\beta\mathcal{H}_{1,n-1}\mathcal{H}_{2,n-1} - p\mathcal{H}_{2,n-1}\mathcal{H}_{3,n-1} - \delta\mathcal{H}_{2,n-1}\right), \\ \mathcal{H}_{3,n+1} = \mathcal{H}_{3,n} &+ \left[\frac{(2-\wp)(1-\wp)}{2} + \frac{3\Delta t}{4}\wp(2-\wp)\right]\left(cp\mathcal{H}_{2,n}\mathcal{H}_{3,n} - \mu\mathcal{H}_{3,n}\right) \\ &- \left[\frac{(2-\wp)(1-\wp)}{2} + \frac{\Delta t}{4}\wp(2-\wp)\right]\left(cp\mathcal{H}_{2,n-1}\mathcal{H}_{3,n-1} - \mu\mathcal{H}_{3,n-1}\right).\end{aligned} \tag{5.15}$$

The results of scheme model (3.3) will be obtained using these explicit iterative schemes.

6. Numerical discussions

A description of the numerical properties of the system is presented in this section. To this end, it is imperative to examine the equilibrium points for the model in more detail.

As mentioned earlier, the positive equilibrium point of

$$\mathcal{P}_i = (\mathcal{H}_1^*, \mathcal{H}_2^*, \mathcal{H}_3^*)$$

for the model is a positive solution for the following system:

$$\begin{aligned} &\tfrac{a\mathcal{H}_1^*}{1+\kappa\mathcal{H}_3^*} - d\mathcal{H}_1^* - b\mathcal{H}_1^*(\mathcal{H}_1^* + \mathcal{H}_2^*) - \beta\mathcal{H}_1^*\mathcal{H}_2^* = 0,\\ &\beta\mathcal{H}_1^*\mathcal{H}_2^* - p\mathcal{H}_2^*\mathcal{H}_3^* - \delta\mathcal{H}_2^* = 0,\\ &cp\mathcal{H}_2^*\mathcal{H}_3^* - \mu\mathcal{H}_3^* = 0. \end{aligned} \tag{6.1}$$

From the last equation of (6.1), we immediately conclude that

$$\mathcal{H}_2^* = \frac{\mu}{cp}. \tag{6.2}$$

Considering this result in the second equation of the system, it reads

$$\mathcal{H}_1^* = \frac{p\mathcal{H}_3^* + \delta}{\beta}. \tag{6.3}$$

Taking these results into account in the first equation of the system along with some simplifications, a quadratic equation for $\mathcal{H}_3^*$ is obtained as

$$C_2\mathcal{H}_3^{*2} + C_1\mathcal{H}_3^* + C_0 = 0, \tag{6.4}$$

where

$$\begin{aligned} C_2 &= bc\kappa\, p^2,\\ C_1 &= bc\delta\kappa p + \beta cd\kappa p + b\beta\kappa\mu + bc\, p^2 + \beta^2\kappa\mu,\\ C_0 &= -a\beta cp + b\delta cp + d\beta cp + b\mu\beta + \beta^2\mu. \end{aligned}$$

The performed numerical simulations in this paper are based on the following parameters:

$$a = 0.5,\ d = 0.1,\ b = 0.1,\ p = 1,\ \delta = 0.2,\ c = 0.8,\ \mu = 0.3,\ \beta = 0.5,\ \kappa = 0.4. \tag{6.5}$$

For these particular choices, the equilibrium point for the model will be determined as follows:

$$(\mathcal{H}_1^{**}, \mathcal{H}_2^{**}, \mathcal{H}_3^{**}) = (1.120356776, 0.375, 0.3601783881)\,. \tag{6.6}$$

In what will come later in this section, the level of sensitivity of the model to the existing parameters will be checked. These results can be considered a confirmation of the theoretical results related to the model.

6.1. *The effects of fractional order ($\wp$)*

Figures 1 and 2 demonstrate the model's sensitivity to the changes of the parameter $\wp$ in the two approximate methods of the article. Convergence of the model to equilibrium point $\left(\mathcal{H}_1^{**}, \mathcal{H}_2^{**}, \mathcal{H}_3^{**}\right)$ is evident in these graphs.

It seems that in Figure 1, for smaller values of $\wp$, the speed of convergence to the balanced point of the system occurs faster, and with its increase, the results will be more unstable and accompanied by fluctuating behavior.

It seems that in Figure 2, the oscillatory behavior increases in the model, and as a result the speed of convergence is very slow.

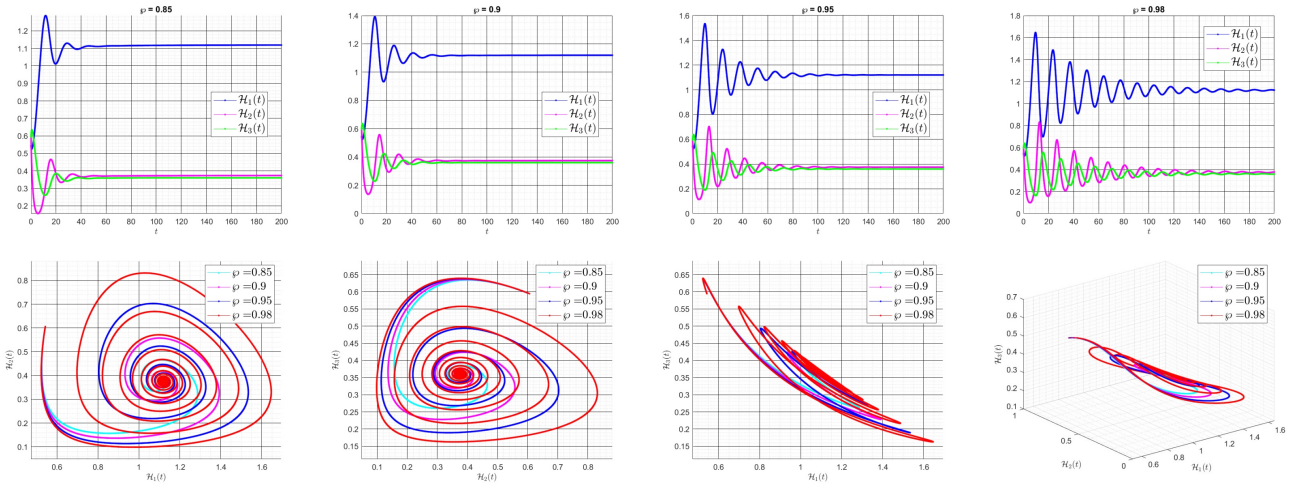

Figure 1. The results of schemes (5.5) and (5.6) obtained from different values of $\wp$.

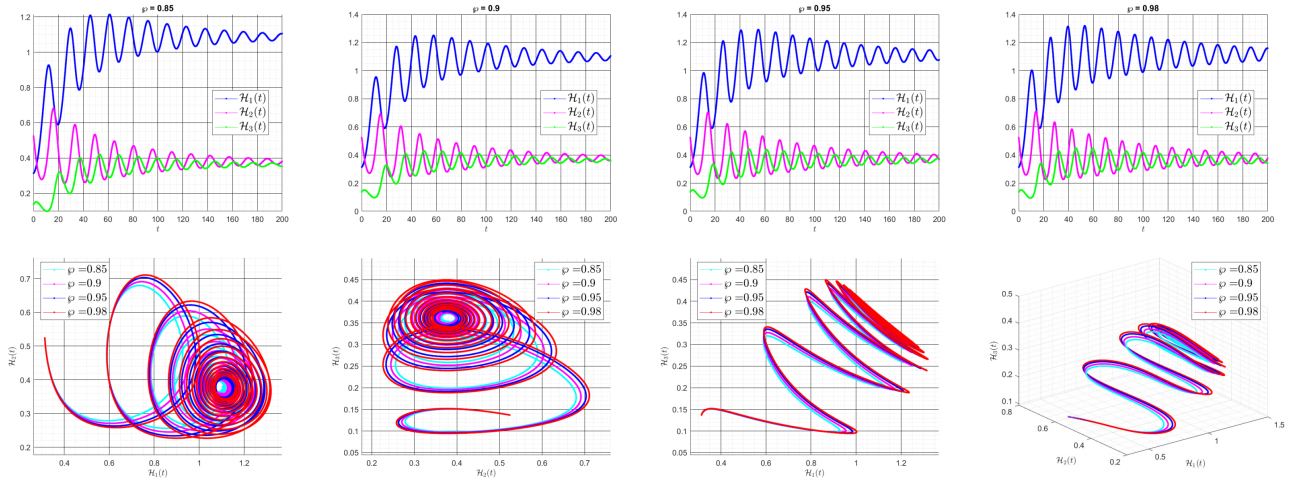

Figure 2. The results of scheme (5.15) obtained from different values of $\wp$.

6.2. *The effects of fear factor (κ)*

The fear parameter (κ) is one of the most important components defined in the model, and it strongly influences the type of system behavior. In [52], a detailed analysis of the effect of this parameter on the

results is presented and can be considered a good benchmark for comparing our results. Figures 3 and 4 demonstrate the model's sensitivity with respect to the changes of parameter κ in the two approximate methods of the article.

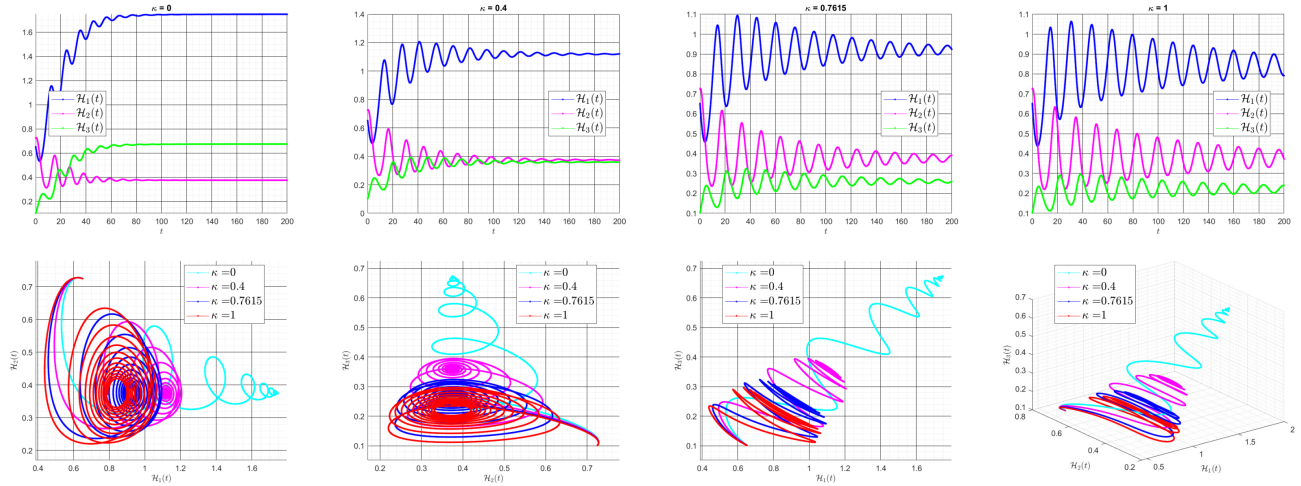

Figure 3. The results of schemes (5.5) and (5.6) obtained from different values of κ together with $\wp = 0.98$.

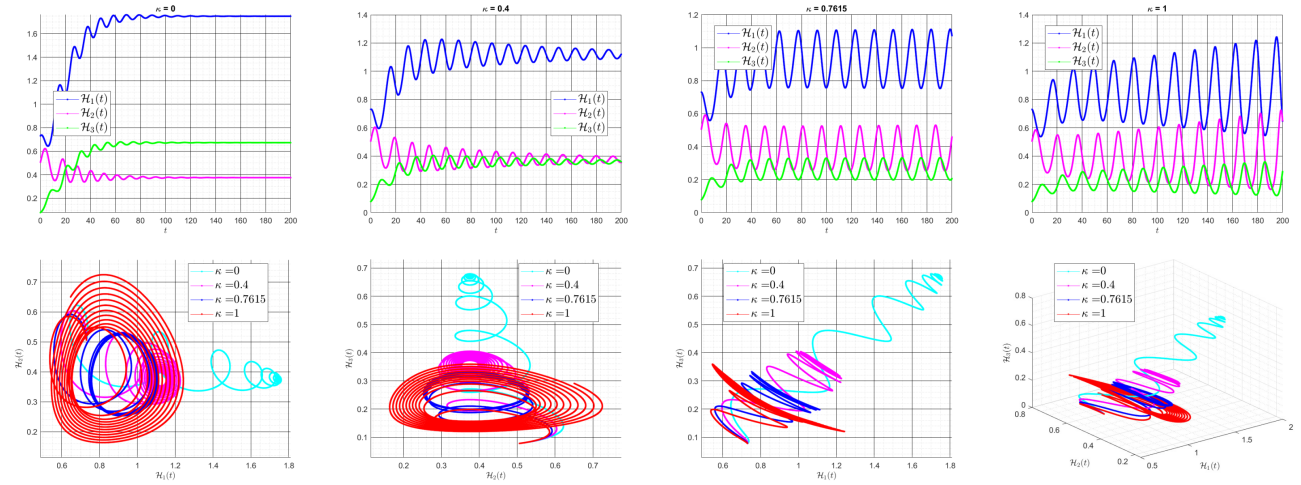

Figure 4. The results of scheme (5.15) obtained from different values of κ together with $\wp = 0.98$.

In this case, the positive equilibrium point is $\left(\frac{p\mathcal{H}_3^*+\delta}{\beta}, \frac{\mu}{cp}, \mathcal{H}_3^*\right)$ where $\mathcal{H}_3^*$ is determined from

$$0.08\kappa\mathcal{H}_3^{*2} + (0.146\kappa + 0.08)\mathcal{H}_3^* - 0.054 = 0. \tag{6.7}$$

In Figures 3 and 4, for $\kappa = 0$, with no fear factor, the equilibrium point of the system is obtained

$$(\mathcal{H}_1^*, \mathcal{H}_2^*, \mathcal{H}_3^*) = (1.75, 0.375, 0.675),$$

whose Jacobian matrix is

$$\mathcal{J}(\mathcal{H}_1^*, \mathcal{H}_2^*, \mathcal{H}_3^*) = \begin{bmatrix} -\frac{7}{40} & -\frac{21}{20} & 0 \\ \frac{3}{16} & 0 & -\frac{3}{8} \\ 0 & \frac{27}{50} & 0 \end{bmatrix}, \tag{6.8}$$

with the following eigenvalues:

$$\begin{bmatrix} -0.09046466345 \\ -0.04226766828 + 0.6244525470\,\mathbf{i} \\ -0.04226766828 - 0.6244525470\,\mathbf{i} \end{bmatrix}.$$

This is a clear proof of the stability of this equilibrium point.

Also, for $\kappa = 0.4$, the equilibrium point of the system is obtained

$$(\mathcal{H}_1^*, \mathcal{H}_2^*, \mathcal{H}_3^*) = (1.120356778, 0.375, 0.360178389),$$

whose Jacobian matrix is

$$\mathcal{J}(\mathcal{H}_1^*, \mathcal{H}_2^*, \mathcal{H}_3^*) = \begin{bmatrix} \frac{-3649+169\sqrt{241}}{1080+520\sqrt{241}} & \frac{471}{200} - \frac{39\sqrt{241}}{200} & \frac{31400-2600\sqrt{241}}{\left(27+13\sqrt{241}\right)^2} \\ \frac{3}{16} & 0 & -\frac{3}{8} \\ 0 & -\frac{173}{100} + \frac{13\sqrt{241}}{100} & 0 \end{bmatrix}, \tag{6.9}$$

with the following eigenvalues:

$$\begin{bmatrix} -0.01004360203 + 0.4818151018\,\mathbf{i} \\ -0.01004360203 - 0.4818151018\,\mathbf{i} \\ -0.09194847354 \end{bmatrix}.$$

With the increase of the real negative parts of the eigenvalues, the instability of the system is gradually increased, which is also clearly evident in the graphs. Finally, for $\kappa = 1$, we have a unique positive equilibrium

$$(\mathcal{H}_1^*, \mathcal{H}_2^*, \mathcal{H}_3^*) = (0.843122550, 0.375, 0.221561275),$$

whose Jacobian matrix is

$$\mathcal{J}(\mathcal{H}_1^*, \mathcal{H}_2^*, \mathcal{H}_3^*) = \begin{bmatrix} \frac{-2029+13\sqrt{17089}}{-1320+40\sqrt{17089}} & \frac{291}{200} - \frac{3\sqrt{17089}}{200} & \frac{7760-80\sqrt{17089}}{\left(-33+\sqrt{17089}\right)^2} \\ \frac{3}{16} & 0 & -\frac{3}{8} \\ 0 & -\frac{113}{100} + \frac{\sqrt{17089}}{100} & 0 \end{bmatrix}, \tag{6.10}$$

with the following eigenvalues:

$$\begin{bmatrix} 0.004096458172 + 0.4025677279\,\mathbf{i} \\ 0.004096458172 - 0.4025677279\,\mathbf{i} \\ -0.09250517127 \end{bmatrix}.$$

So, a clear proof of the instability of this equilibrium point is observed.

The numerical results obtained in this case are completely consistent with the numerical properties reported in [52].

6.3. *The effects of the contact rate between the susceptible and the infected prey (β)*

Figures 5 and 6 demonstrate the model's sensitivity with respect to the changes of parameter β in the two approximate methods of the article.

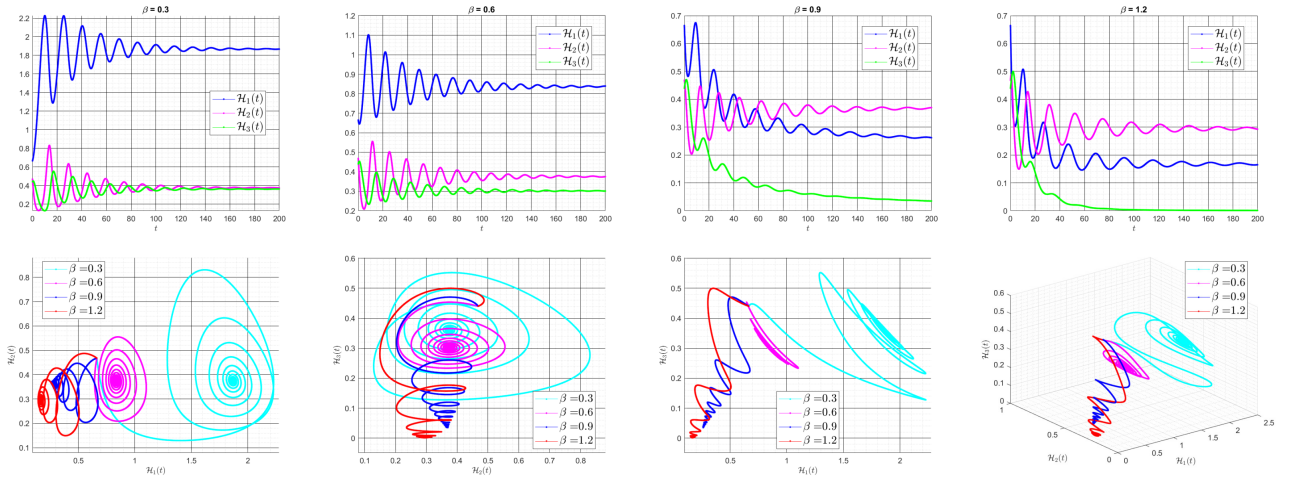

Figure 5. The results of schemes (5.5) and (5.6) obtained from different values of β together with $\wp = 0.98$.

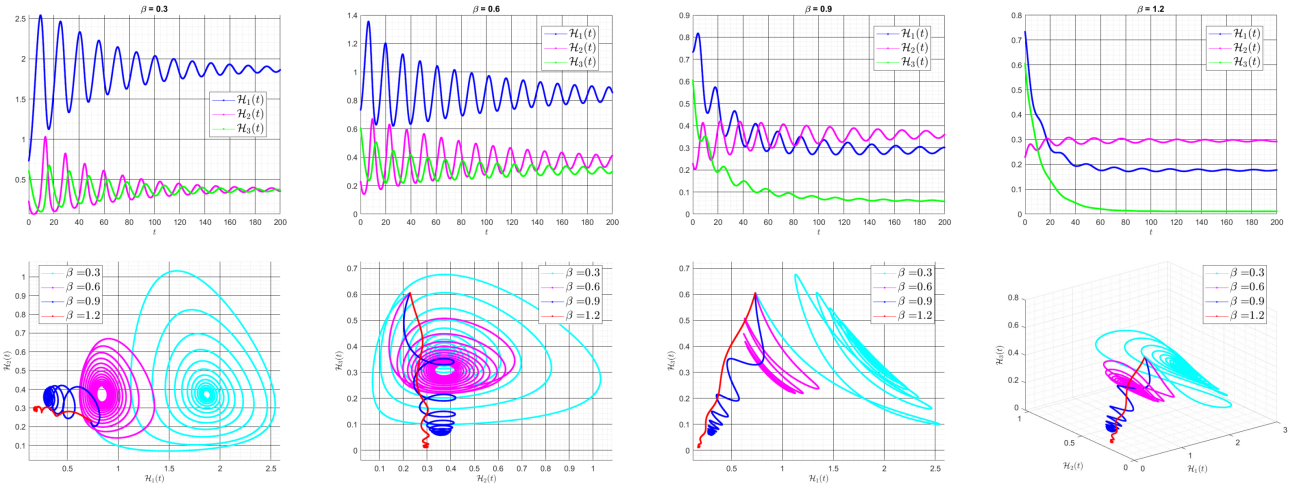

Figure 6. The results of scheme (5.15) obtained from different values of β together with $\wp = 0.98$.

In these diagrams, it can be seen that as β increases, the equilibrium type changes from an interior point to a planar point. For these situations, the infected predator population is on the way to extinction. For example, for $\beta = 1.2$, we have a unique positive equilibrium

$$(\mathcal{H}_1^*, \mathcal{H}_2^*, \mathcal{H}_3^*) = (0.1666666667, 0.2948717949, 0),$$

whose Jacobian matrix is

$$\mathcal{J}(\mathcal{H}_1^*, \mathcal{H}_2^*, \mathcal{H}_3^*) = \begin{bmatrix} -0.0166666667 & -0.2166666667 & -0.03333333334 \\ 0.3538461539 & 0.0 & -0.2948717949 \\ 0 & 0.0 & -0.0641025641 \end{bmatrix}, \tag{6.11}$$

with the following eigenvalues:

$$\begin{bmatrix} -0.008333333350 + 0.2767620318\,\mathbf{i} \\ -0.008333333350 - 0.2767620318\,\mathbf{i} \\ -0.06410256410 \end{bmatrix}.$$

6.4. The effects of the attack rate on the infected prey (p)

Figures 7 and 8 demonstrate the model's sensitivity with respect to the changes of the attack rate on the infected prey in the two approximate methods of the article.

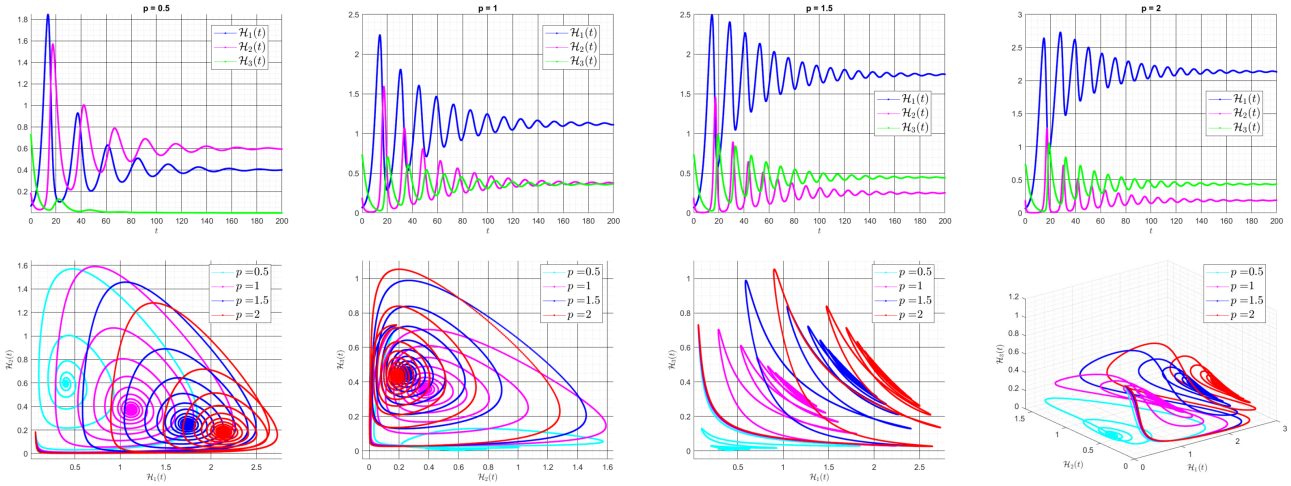

Figure 7. The results of schemes (5.5) and (5.6) obtained from different values of p together with $\wp = 0.98$.

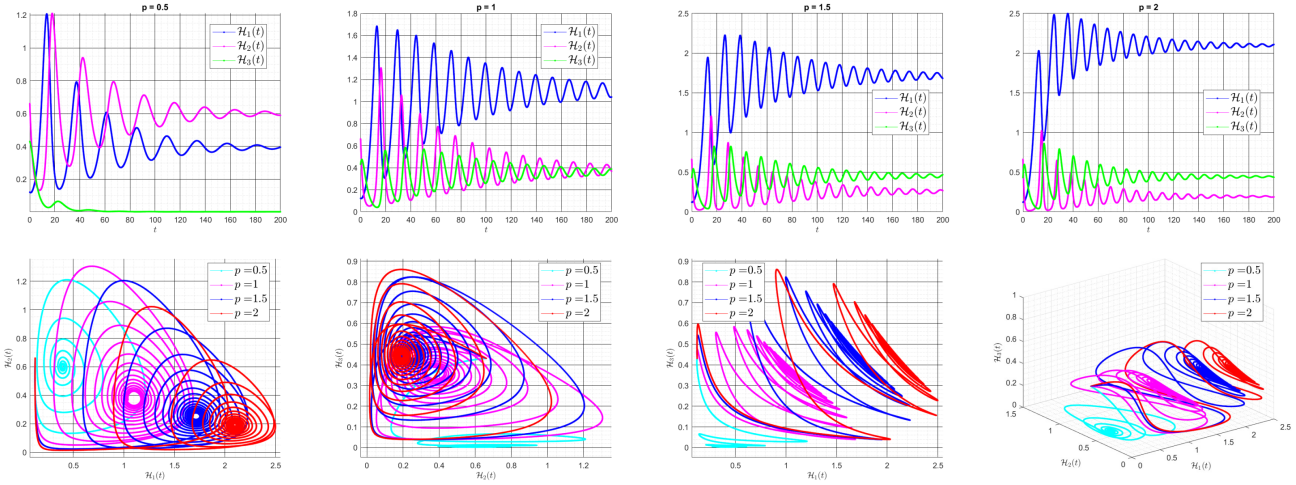

Figure 8. The results of scheme (5.15) obtained from different values of p together with $\wp = 0.98$.

The important thing that can be seen from the results is that with the increase of the value for the parameter, the type of equilibrium point in the problem changes completely.

7. Conclusions

The models in eco-epidemiology are computational tools that describe ecology and epidemiology problems in a meaningful way. The use of novel mathematical definitions in modeling eco-epidemiological scenarios can be very helpful and lead to significant results in real-world problems. The aim of this paper is to study a nonlinear predator-prey system where the prey growth rate is reduced due to anti-predator behavior. This paper employs two new definitions in fractional calculus called the ABC and CFC fractional derivatives. These two definitions are useful tools that can be used for solving the model. Our research results may be of great value to scholars in the future, when they want to apply our employed techniques to model real problems related to the epidemic and control it more efficiently.

Acknowledgments

The authors extend their appreciation to Prince Sattam bin Abdulaziz University for funding this research work through the project number (PSAU/2023/01/23035).

Conflict of interest

The authors declare that they have no competing interests.

References

1. B. Ghanbari, D. Baleanu, Applications of two novel techniques in finding optical soliton solutions of modified nonlinear Schrödinger equations, *Results Phys.*, **44** (2023), 106171. http://doi.org/10.1016/j.rinp.2022.106171
2. C. Huang, Z. Han, M. Li, X. Wang, W. Zhao, Sentiment evolution with interaction levels in blended learning environments: using learning analytics and epistemic network analysis, *Australas. J. Educ. Technol.*, **37** (2021), 81–95. http://doi.org/10.14742/ajet.6749
3. S. Lu, B. Yang, Y. Xiao, S. Liu, M. Liu, L. Yin, et al., Iterative reconstruction of low-dose CT based on differential sparse, *Biomed. Signal Process. Control*, **79** (2023), 104204. http://doi.org/10.1016/j.bspc.2022.104204
4. D. Baleanu, A. Jajarmi, H. Mohammadi, S. Rezapour, A new study on the mathematical modelling of human liver with Caputo-Fabrizio fractional derivative, *Chaos Solitons Fract.*, **134** (2020), 109705. http://doi.org/10.1016/j.chaos.2020.109705
5. Y. Ban, Y. Wang, S. Liu, B. Yang, M. Liu, L. Yin, et al., 2D/3D multimode medical image alignment based on spatial histograms, *Appl. Sci.*, **12** (2022), 8261. http://doi.org/10.3390/app12168261
6. X. Qin, Y. Ban, P. Wu, B. Yang, S. Liu, L. Yin, et al., Improved image fusion method based on sparse decomposition, *Electronics*, **11** (2022), 2321. http://doi.org/10.3390/electronics11152321

7. H. Liu, M. Liu, D. Li, W. Zheng, L. Yin, R. Wang, Recent advances in pulse-coupled neural networks with applications in image processing, *Electronics*, **11** (2022), 3264. http://doi.org/10.3390/electronics11203264
8. H. Mohammadi, S. Kumar, S. Rezapour, S. Etemad, A theoretical study of the Caputo-Fabrizio fractional modeling for hearing loss due to Mumps virus with optimal control, *Chaos Solitons Fract.*, **144** (2021), 110668. http://doi.org/10.1016/j.chaos.2021.110668
9. H. Li, R. Peng, Z. Wang, On a diffusive susceptible-infected-susceptible epidemic model with mass action mechanism and birth-death effect: analysis, simulations, and comparison with other mechanisms, *SIAM J. Appl. Math.*, **78** (2018), 2129–2153. http://doi.org/10.1137/18M1167863
10. W. Lyu, Z. Wang, Logistic damping effect in chemotaxis models with density-suppressed motility, *Adv. Nonlinear Anal.*, **12** (2022), 336–355. http://doi.org/10.1515/anona-2022-0263
11. H. Y. Jin, Z. A. Wang, Asymptotic dynamics of the one-dimensional attraction–repulsion Keller–Segel model, *Math. Methods Appl. Sci.*, **38** (2015), 444–457. http://doi.org/10.1002/mma.3080
12. R. Ye, P. Liu, K. Shi, B. Yan, State damping control: a novel simple method of rotor UAV with high performance, *IEEE Access*, **8** (2020), 214346–214357. http://doi.org/10.1109/ACCESS.2020.3040779
13. Q. Zeng, B. Bie, Q. Guo, Y. Yuan, Q. Han, X. Han, et al., Hyperpolarized Xe NMR signal advancement by metal-organic framework entrapment in aqueous solution, *Proc. Natl. Acad. Sci.*, **117** (2020), 17558–17563. http://doi.org/10.1073/pnas.2004121117
14. X. Zhang, Y. Qu, L. Liu, Y. Qiao, H. Geng, Y. Lin, et al., Homocysteine inhibits pro-insulin receptor cleavage and causes insulin resistance via protein cysteine-homocysteinylation, *Cell Rep.*, **37** (2021), 109821. http://doi.org/10.1016/j.celrep.2021.109821
15. M. Wang, L. Deng, G. Liu, L. Wen, J. Wang, K. Huang, et al., Porous organic polymer-derived nanopalladium catalysts for chemoselective synthesis of antitumor benzofuro [2,3-*b*] pyrazine from 2-bromophenol and isonitriles, *Org. Lett.*, **21** (2019), 4929–4932. http://doi.org/10.1021/acs.orglett.9b01230
16. M. Cheng, Y. Cui, X. Yan, R. Zhang, J. Wang, X. Wang, Effect of dual-modified cassava starches on intelligent packaging films containing red cabbage extracts, *Food Hydrocolloids*, **124** (2022), 107225. http://doi.org/10.1016/j.foodhyd.2021.107225
17. N. H. Tuan, H. Mohammadi, S. Rezapour, A mathematical model for COVID-19 transmission by using the Caputo fractional derivative, *Chaos Solitons Fract.*, **140** (2020), 110107. http://doi.org/10.1016/j.chaos.2020.110107
18. O. Yuan, B. Kato, K. Fan, Y. Wang, Phased array guided wave propagation in curved plates, *Mech. Syst. Signal Process.*, **185** (2023), 109821. http://doi.org/10.1016/j.ymssp.2022.109821
19. Q. Shen, Z. Yang, Applied mathematical analysis of organizational learning culture and new media technology acceptance based on regression statistical software and a moderated mediator model, *J. Comput. Methods Sci. Eng.*, **21** (2021), 1825–1842. http://doi.org/10.3233/JCM-215455
20. Z. Lv, Z. Yu, S. Xie, A. Alamri, Deep learning-based smart predictive evaluation for interactive multimedia-enabled smart healthcare, *ACM Trans. Multimedia Comput. Commun. Appl.*, **18** (2022), 1–20. http://doi.org/10.1145/3468506

21. H. Y Jin, Z. A. Wang, Boundedness, blowup and critical mass phenomenon in competing chemotaxis, *J. Differ. Equations*, **260** (2016), 162–196. http://doi.org/10.1016/j.jde.2015.08.040

22. J. Wang, D. Wu, Y. Gao, X. Wang, X. Li, G. Xu, et al., Integral real-time locomotion mode recognition based on GA-CNN for lower limb exoskeleton, *J. Bionic Eng.*, **19** (2022), 1359–1373. http://doi.org/10.1007/s42235-022-00230-z

23. X. Xie, B. Xie, D. Xiong, M. Hou, J. Zuo, G. Wei, et al., New theoretical ISM-K2 Bayesian network model for evaluating vaccination effectiveness, *J. Ambient Intell. Humaniz Comput.*, **2022** (2022), 1–17. http://doi.org/10.1007/s12652-022-04199-9

24. X. Xie, T. Wang, W. Zhang, Existence of solutions for the (p, q)-Laplacian equation with nonlocal Choquard reaction, *Appl. Math. Lett.*, **135** (2023), 108418. http://doi.org/10.1016/j.aml.2022.108418

25. F. Wang, H. Wang, X. Zhou, R. Fu, A driving fatigue feature detection method based on multifractal theory, *IEEE Sens. J.*, **22** (2022), 19046–19059. http://doi.org/10.1109/JSEN.2022.3201015

26. X. Xie, B. Xie, J. Cheng, Q. Chu, T. Dooling, A simple Monte Carlo method for estimating the chance of a cyclone impact, *Nat. Hazards*, **107** (2021), 2573–2582. http://doi.org/10.1007/s11069-021-04505-2

27. Y. Liu, K. D. Xu, J. Li, Y. J. Guo, A. Zhang, Q. Chen, Millimeter-wave E-plane waveguide bandpass filters based on spoof surface plasmon polaritons, *IEEE Trans. Microw. Theory Tech.*, **70** (2022), 4399–4409. http://doi.org/10.1109/TMTT.2022.3197593

28. K. D. Xu, Y. J. Guo, Y. Liu, X. Deng, Q. Chen, Z. Ma, 60-GHz compact dual-mode on-chip bandpass filter using GaAs technology, *IEEE Electron Device Lett.*, **42** (2021), 1120–1123. http://doi.org/10.1109/LED.2021.3091277

29. B. Dai, B. Zhang, Z. Niu, Y. Feng, Y. Liu, Y. Fan, A novel ultrawideband branch waveguide coupler with low amplitude imbalance, *IEEE Trans. Microw. Theory Tech.*, **70** (2022), 3838–3846. http://doi.org/10.1109/TMTT.2022.3186326

30. Y. Feng, B. Zhang, Y. Liu, Z. Niu, Y. Fan, X. Chen, A D-band manifold triplexer with high isolation utilizing novel waveguide dual-mode filters, *IEEE Trans. Terahertz Sci. Technol.*, **12** (2022), 678–681. http://doi.org/10.1109/TTHZ.2022.3203308

31. J. Li, Y. Zhao, A. Zhang, B. Song, R. L. Hill, Effect of grazing exclusion on nitrous oxide emissions during freeze-thaw cycles in a typical steppe of Inner Mongolia, *Agric. Ecosyst Environ.*, **307** (2021), 107217. http://doi.org/10.1016/j.agee.2020.107217

32. X. Wang, Y. Zhang, M. Luo, K. Xiao, Q. Wang, Y. Tian, et al., Radium and nitrogen isotopes tracing fluxes and sources of submarine groundwater discharge driven nitrate in an urbanized coastal area, *Sci. Total Environ.*, **763** (2021), 144616. http://doi.org/10.1016/j.scitotenv.2020.144616

33. Z. Wang, L. Dai, J. Yao, T. Guo, D. Hrynsphan, S. Tatsiana, et al., Improvement of Alcaligenes sp. TB performance by Fe-Pd/multi-walled carbon nanotubes: enriched denitrification pathways and accelerated electron transport, *Bioresour. Technol.*, **327** (2021), 124785. http://doi.org/10.1016/j.biortech.2021.124785

34. Z. Zhang, P. Ma, R. Ahmed, J. Wang, D. Akin, F. Soto, et al., Advanced point-of-care testing technologies for human acute respiratory virus detection, *Adv Mater.*, **34** (2022), 2103646. http://doi.org/10.1002/adma.202103646

35. H. Chen, Q. Wang, Regulatory mechanisms of lipid biosynthesis in microalgae, *Biol. Rev.*, **96** (2021), 2373–2391. http://doi.org/10.1111/brv.12759

36. W. Zheng, Y. Xun, X. Wu, Z. Deng, X. Chen, Y. Sui, A comparative study of class rebalancing methods for security bug report classification, *IEEE Trans. Reliab.*, **70** (2021), 1658–1670. http://doi.org/10.1109/TR.2021.3118026

37. H. Kong, L. Lu, J. Yu, Y. Chen, F. Tang, Continuous authentication through finger gesture interaction for smart homes using WiFi, *IEEE Trans. Mobile Comput.*, **20** (2020), 3148–3162. http://doi.org/10.1109/TMC.2020.2994955

38. C. Li, L. Lin, L. Zhang, R. Xu, X. Chen, J. Ji, et al., Long noncoding RNA p21 enhances autophagy to alleviate endothelial progenitor cells damage and promote endothelial repair in hypertension through SESN2/AMPK/TSC2 pathway, *Pharmacol. Res.*, **173** (2021), 105920. http://doi.org/10.1016/j.phrs.2021.105920

39. H. Gao, P. H. Hsu, K. Li, J. Zhang, The real effect of smoking bans: evidence from corporate innovation, *J. Financ. Quant. Anal.*, **55** (2020), 387–427. http://doi.org/10.1017/S0022109018001564

40. A. K. Alzahrani, A. S. Alshomrani, N. Pal, S. Samanta, Study of an eco-epidemiological model with Z-type control, *Chaos Solitons Fract.*, **113** (2018), 197–208. http://doi.org/10.1016/j.chaos.2018.06.012

41. B. Ghanbari, On approximate solutions for a fractional prey–predator model involving the Atangana-Baleanu derivative, *Adv. Differ. Equations*, **2020** (2020), 679. http://doi.org/10.1186/s13662-020-03140-8

42. B. Ghanbari, S. Djilali, Mathematical and numerical analysis of a three-species predator-prey model with herd behavior and time fractional-order derivative, *Math. Methods Appl. Sci.*, **43** (2019), 1736–1752. http://doi.org/10.1002/mma.5999

43. Y. Chu, M. F. Khan, S. Ullah, S. A. A. Shah, M. Farooq, M. bin Mamat, Mathematical assessment of a fractional-order vector–host disease model with the Caputo-Fabrizio derivative, *Math. Methods Appl. Sci.*, **46** (2022), 232–247. http://doi.org/10.1002/mma.8507

44. W. Shen, Y. Chu, M. ur Rahman, I. Mahariq, A. Zeb, Mathematical analysis of HBV and HCV co-infection model under nonsingular fractional order derivative, *Results Phys.*, **28** (2021), 104582. http://doi.org/10.1016/j.rinp.2021.104582

45. B. Ghanbari, Chaotic behaviors of the prevalence of an infectious disease in a prey and predator system using fractional derivatives, *Math. Methods Appl. Sci.*, **44** (2021), 9998–10013. http://doi.org/10.1002/mma.7386

46. H. Jin, Z. Wang, L. Wu, Global dynamics of a three-species spatial food chain model. *J. Differ. Equations*, **333** (2022), 144–183. http://doi.org/10.1016/j.jde.2022.06.007

47. B. Ghanbari, A fractional system of delay differential equation with nonsingular kernels in modeling hand-foot-mouth disease, *Adv. Differ. Equations*, **2020** (2020), 536. http://doi.org/10.1186/s13662-020-02993-3

48. A. Atangana, D. Baleanu, New fractional derivatives with nonlocal and non-singular kernel: theory and application to heat transfer model, *Therm. Sci.*, **20** (2016), 763–769. http://doi.org/10.2298/TSCI160111018A

49. K. Diethelm, R. Garrappa, A. Giusti, M. Stynes, Why fractional derivatives with nonsingular kernels should not be used, *Fractional Calculus Appl. Anal.*, **23** (2023), 610–634. http://doi.org/10.1515/fca-2020-0032

50. I. Podlubny, *Fractional differential equations: an introduction to fractional derivatives, fractional differential equations, to methods of their solution and some of their applications*, Elsevier, 1999.

51. M. Caputo, M. Fabrizio, A new definition of fractional derivative without singular kernel, *Progr. Fract. Differ. Appl.*, **1** (2015), 73–85. http://doi.org/10.12785/pfda/010201

52. Y. Tan, Y. Cai, R. Yao, M. Hu, E. Wang, Complex dynamics in an eco-epidemiological model with the cost of anti-predator behaviors, *Nonlinear Dyn.*, **107** (2022), 3127–3141. http://doi.org/10.1007/s11071-021-07133-4

53. R. Garrappa, Numerical solution of fractional differential equations: a survey and a software tutorial, *Mathematics*, **6** (2018), 16. http://doi.org/10.3390/math6020016

54. B. Ghanbari, D. Kumar, Numerical solution of predator-prey model with Beddington-DeAngelis functional response and fractional derivatives with Mittag-Leffler kernel, *Chaos*, **29** (2019), 063103. http://doi.org/10.1063/1.5094546

55. B. Ghanbari, C. Cattani, On fractional predator and prey models with mutualistic predation including non-local and nonsingular kernels, *Chaos Solitons Fract.*, **136** (2020), 109823. http://doi.org/10.1016/j.chaos.2020.109823

56. B. Ghanbari, S. Kumar, R. Kumar, A study of behaviour for immune and tumor cells in immunogenetic tumour model with non-singular fractional derivative, *Chaos Solitons Fract.*, **133** (2020), 109619. http://doi.org/10.1016/j.chaos.2020.109619

57. B. Ghanbari, On fractional approaches to the dynamics of a SARS-CoV-2 infection model including singular and non-singular kernels, *Results Phys.*, **28** (2021), 104600. http://doi.org/10.1016/j.rinp.2021.104600

AIMS Press